Quantum Electronics **36** (5) 464 – 469 (2006)

OPTICAL FIBRES

PACS numbers: 42.81.Dp; 42.25.Fx
DOI: 10.1070/QE2006v036n05ABEH013159

Study of the radiation scattering indicatrix in fibres heavily doped with germanium oxide

M.E. Likhachev, M.M. Bubnov, S.L. Semjonov, V.F. Khopin, M.Yu. Salganskii, A.N. Gur'yanov, E.M. Dianov

***Abstract*. The original setup for measuring the radiation scattering indicatrix in a broad angular range from 1 to 179° is developed. It is shown experimentally that total optical losses in single-mode fibres heavily doped with germanium oxide are determined by optical losses caused by fundamental mechanisms and by anomalous scattering. The analysis of the anomalous scattering indicatrix and the spectral dependence of excess optical losses showed that anomalous scattering is caused by scattering from fluctuations of the fibre core – cladding interface along the fibre length. The mechanism of these fluctuations is proposed and substantiated.**

Keywords: *fibre optics, heavily doped fibres, germanosilicate fibre, optical losses, light scattering, Rayleigh scattering*.

1. Introduction

Single-mode optical fibres heavily doped with germanium oxide (up to molar concentration 15 % – 30 %) are key elements in a number of nonlinear devices [1 – 3]. The increase in the molar concentration of GeO_2 from 3 % – 5 % (standard for single-mode fibres used in communication links) up to 30 % and the corresponding decrease in the core diameter leads to the increase in the fibre nonlinearity by more than an order of magnitude. At the same time, total optical losses drastically increase and it substantially reduces the efficiency of devices based on such fibres. Thus, optical losses at a wavelength of 1.55 μm in single-mode fibres manufactured by the MCVD method increase from 0.2 dB km^{-1} up to 2 – 5 dB km^{-1} with increasing the molar concentration of germanium oxide in the fibre core from 3 % to 30 % [3, 4]. Only recently, by optimising the refractive index profile and the fibre drawing conditions, we have managed to reduce optical losses down to 1.33 dB km^{-1} at the molar concentration of GeO_2 in the fibre core equal to 29 % [5, 6].

In modern lowly doped single-mode and multimode fibres used in optical communication systems, optical losses are mainly determined by Rayleigh scattering [7, 8]. To explain the nature of optical losses in heavily doped single-mode fibres, a number of hypotheses were proposed. The authors of some studies [2, 4, 6, 9 – 12] argue that optical losses in these fibres are mainly determined by scattering. On the other hand, the authors of other papers [13 – 16] explain a high level of optical losses in heavily doped single-mode fibres by excess absorption. The study of the scattering indicatrix [6, 10 – 12] showed the presence of additional light scattering in heavily doped fibres, which was different from Rayleigh scattering. This type of scattering, which was first discovered in weakly doped fibres [9], has the asymmetrical indicatrix whose amplitude is significant only at small angles to the fibre axis in the propagation direction of probe radiation. According to [11], we will call below this type of scattering anomalous. Because the angular range of measurements of the scattering radiation intensity was restricted in each of the above-mentioned papers (20 – 160° [10], 10 – 170° [11], and 1 – 16° [6, 12]), the authors have failed to determine accurately the contribution of anomalous scattering to the total optical losses of the fibres. Note also that the authors of paper [11] mainly studied few-mode fibres, which does not allow one to determine the contribution of scattering to total optical losses in single-mode fibres in the near IR range.

In this paper, we present the results of investigations performed on a new experimental setup. We measured the intensity of scattered light in a broad angular range and determined quite accurately the contribution of anomalous scattering to optical losses. Based on these data, we propose the mechanism of this scattering.

2. Setup for measuring the angular dependence of the scattered light intensity

The scheme of the experimental setup for measuring the angular dependence of the scattered light intensity in optical fibres is presented in Fig. 1. The fibre under study was placed on a silica glass plate and covered with a silica prism. By means of diaphragms deposited on the plate and prism (scheme 1), all the types of irradiation were eliminated except radiation scattered in a small (of length ~ 4 cm) emitting region of the fibre with a polymer coating removed. Scheme 1 was used for measuring the intensity of

M.E. Likhachev, M.M. Bubnov, S.L. Semjonov, E.M. Dianov Fiber Optics Research Center, A.M. Prokhorov General Physics Institute, Russian Academy of Sciences, ul. Vavilova 38, 119991 Moscow, Russia; e-mail: likhachev@fo.gpi.ru;
V.F. Khopin, M.Yu. Salganskii, A.N. Gur'yanov Institute of Chemistry of High-Purity Substances, Russian Academy of Sciences, ul. Tropinina 49, 603600 Nizhnii Novgorod, Russia; e-mail: vkhopin@mail.ru

Received 7 April 2006
Kvantovaya Elektronika **36** (5) 464 – 469 (2006)
Translated by M.N. Sapozhnikov

radiation scattered at angles 1 – 30° and 150 – 179°. The radiation scattered in the fibre reflected from a mirror deposited on one of the prism surfaces, and the beams leaving the fibre at the same angle were focused with the lens to a point in the focal plane. The radiation propagating from the fibre directly to the focal plane was removed in scheme 1.

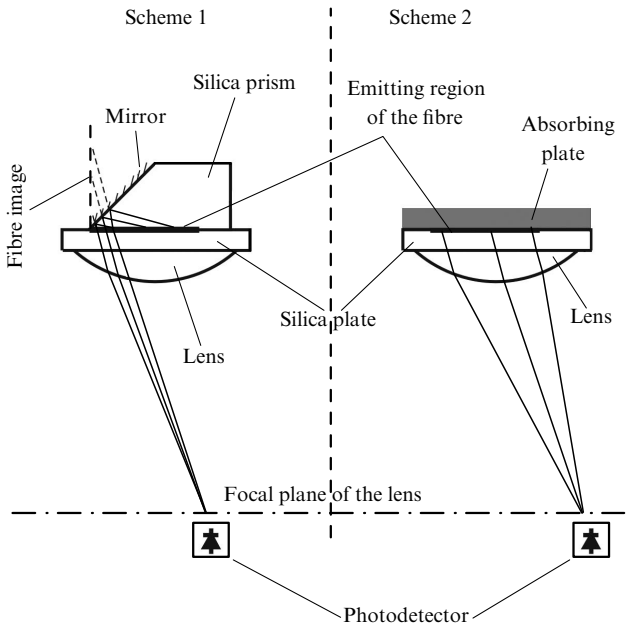

Figure 1. Schemes of setups for measuring the angular distribution of the radiation intensity scattered in a fibre.

Scheme 2 was used for measuring the distribution of the scattered light intensity in the angular range from 60 to 120°. An absorbing plate was placed over the emitting region of the fibre, and the intensity of radiation propagating directly from the fibre to the focal plane was measured.

The radiation intensity measured in experiments was normalised by means of multimode fibres, where Rayleigh scattering of light occurs in a broad angular range. The absolute intensity of Rayleigh scattering in these fibres was determined from the measured dependences of Rayleigh scattering coefficients on the concentration of germanium oxide [8, 17 – 19].

The output end of the fibre was placed into an immersion liquid with the refractive index close to that of silica glass. This procedure was necessary because radiation reflected back from the output end distorted somewhat the scattered light intensity indicatrix.

Measurements were performed at the wavelength 1.064 μm of a Nd : YAG laser with linearly polarised radiation. Because the scattering intensity can be sensitive to the direction of polarisation (in particular, in the case of Rayleigh scattering), the measurements were performed in two planes perpendicular and parallel to the radiation polarisation, and then the results of measurements were averaged. For each fibre, measurements were performed for three different regions, and the results were also averaged.

3. Experimental results

3.1 Angular distribution of scattered radiation. Contribution of scattering to total optical losses

To study the angular distribution of scattered radiation in heavily doped fibres, we fabricated two fibre preforms Nos 304 and 325. Both preforms had step-index profiles formed by the addition of germanium oxide into the fibre core. The refractive index difference Δn between the fibre core and cladding for preforms Nos 304 and 325 was 0.040 and 0.025, respectively. Optical fibres of diameter 125 μm were drawn from each preform in four regimes at different temperatures and different drawing rates.

Figure 2 presents the typical dependence of the scattered light intensity on the scattering angle in the reflecting cladding for fibre No. 325 ($\Delta n = 0.025$) drawn at the temperature 1880 °C at the rate 60 m min^{-1}. The dotted curve shows the approximation of the scattered light intensity in the angular range where measurements were not performed. Also, the calculated level of Rayleigh scattering is shown by the dashed curve. The deviation of the angular intensity distribution of Rayleigh scattering at small angles to the fibre axis from the relation

$$I_R = \frac{1}{2} I_0 (1 + \cos^2 \varphi) \qquad (1)$$

is caused by a partial capture of scattered light by the fibre core, which was taken into account in the calculation of the theoretical curve (radiation entering the aperture of the heavily doped fibre core does not escape through the side surface of the fibre and therefore is neglected, whereas the refraction of the rest of radiation at the fibre core – cladding interface is taken into account).

The intensity of scattering in all fibres measured in a broad angular range (0 – 70°) was noticeably higher than the Rayleigh scattering intensity. The maximum scattering intensity was observed at small angles to the fibre axis in

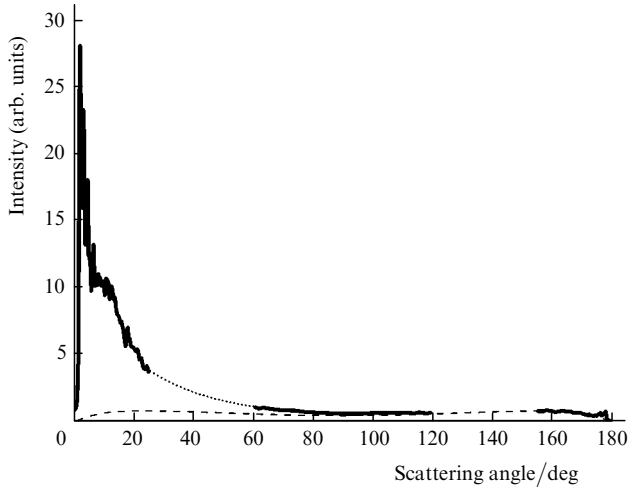

Figure 2. Angular distribution of the scattered light intensity in a single-mode fibre drawn at the temperature 1880 °C from preform No. 325. The dashed curve shows the calculated level of Rayleigh scattering; the dotted curve is the approximation of the scattering indicatrix in the angular range where measurements were not performed.

the propagation direction of probe radiation. The shape of the scattering indicatrix reveals the presence of anomalous scattering in the fibres, which was earlier observed in papers [6, 9–12].

Indicatrix measurements allow us to determine contribution of scattering to the total losses in fibres under study. The UV absorption was estimated as 0.45 and 0.3 dB km^{-1} at 1.06 μm [2, 20] for fibres drawn from preforms Nos 304 and 325, respectively. The IR absorption in these fibres at 1.06 μm was a few orders of magnitude lower than 1 dB km^{-1} [8] and therefore was neglected. The total optical losses at 1.06 μm were determined by the cut-back method. Figure 3 shows the dependence of total optical losses, obtained by summation of estimated optical losses due to scattering and absorption, on the tension upon fibre drawing, as well as the corresponding dependence for optical losses determined by the cut-back method. The results of measurements are presented in Table 1. The error of measuring optical losses by the cut-back method was about 5 % and the scatter of estimates made from the measurements of the scattering indicatrix was about 10 %.

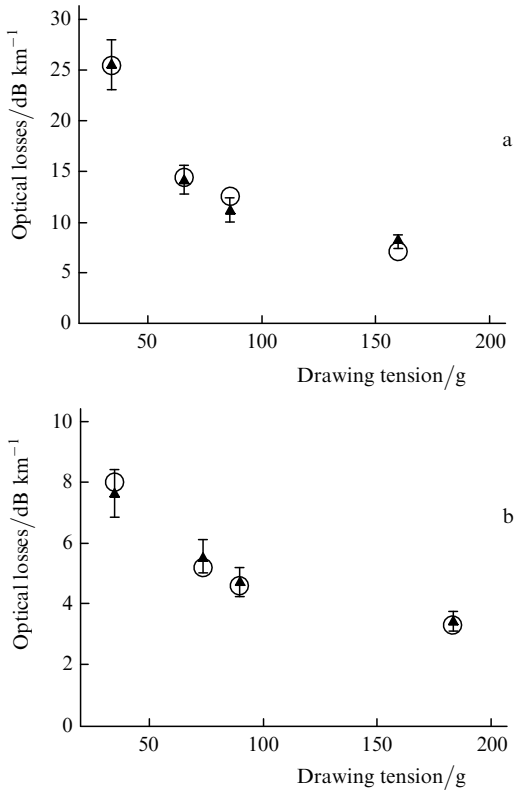

Figure 3. Dependences of optical losses on tension in fibres drawn from preforms No. 304 (a) and No. 325 (b); circles are total optical losses (cut-back method), triangles are the sum of optical losses caused by fundamental mechanisms and anomalous scattering.

The results presented above show that total optical losses due to fundamental mechanisms and anomalous scattering coincide within the error of 10 % with total optical losses measured by the standard method. The total optical losses in all the fibres are mainly determined by scattering. It is interesting to note that optical losses in fibres drawn at the same temperature but at different rates are substantially different. At the same time, fibres drawn at different temperatures and different rates, but with approximately the same tension, have close optical losses. One can see from Fig. 3 that, as the tension is increased during fibre drawing, optical losses decrease monotonically, which means that they are directly related to the tension strength.

3.2 Mechanism of anomalous scattering

We showed above that the excess (different from fundamental) optical losses in heavily doped single-mode fibres are related to anomalous scattering. We have found earlier [22] that the sources of excess optical losses in heavily doped germanosilicate fibres are located at the core–cladding interface. This means that the source of anomalous scattering of light is the fibre core–cladding interface.

In [23], a model of light scattering by spatial fluctuations of the core–cladding interface along the fibre length was proposed. It was shown that such scattering mainly occurs at small angles (2–20°) to the fibre axis in the propagation direction of probe radiation. In this case, the characteristic size of variations in the core–cladding interface in the azimuthal and axial directions should be comparable with the wavelength of scattered radiation or exceed it, while in the radial direction this size should be far smaller than this wavelength. Later [24], this model was extended to the case of the stochastic distribution of azimuthal and radial fluctuations and the expression

$$P(\theta) = \frac{k^4\sigma^2 a^2 \Delta^4}{2\pi^3}\left(\frac{n_0 c E_a^2}{8\pi}\right)(1+\cos^2\theta)T(\theta)\times$$

$$\times \int_0^L (L-u)R(u)\cos[k(\cos\theta-1)u]\mathrm{d}u$$

Table 1. Total optical losses and scattering losses at a wavelength of 1.064 μm measured in fibres drawn from preforms Nos 304 and 325.

Preform number	Parameters of the fibre drawing			Optical losses				
	T/°C	v/m s^{-1}	τ/g	α_{scat}/dB km^{-1}	α_{UV}/dB km^{-1}	α_R/dB km^{-1}	α_Σ/dB km^{-1} (estimate)	α_{tot}/dB km^{-1} (measurement)
304	1880	1	160	6.9	0.45	1.63	7.35	7.0
	1880	0.5	86	9.64	0.45	1.92	10.1	12.2
	1940	1	66	12.5	0.45	2.05	13.0	14.0
	1940	0.5	34	22.9	0.45	2.37	23.4	25.0
325	1880	1	184	3	0.3	1.15	3.3	3.18
	1880	0.5	90	4.1	0.3	1.19	4.4	4.49
	1940	1	74	4.9	0.3	1.24	5.2	5.16
	1940	0.5	35	7.1	0.3	1.31	7.4	7.73

Notes. T is the heater temperature; v is the drawing rate; τ is the average tension in grams (determined by the contactless method during fibre drawing before the application of a polymer coating), α_R is Rayleigh scattering (backward scattering method [18, 21]); α_{UV} is UV absorption (estimated from [2, 20]); α_{scat} are total losses caused by scatterings of all types (from the scattering indicatrix); α_Σ is the estimated sum of scattering (α_{scat}) and absorption (α_{UV}) losses; α_{tot} is losses measured by the cut-back method.

$$\times \int_0^{\pi\sqrt{2}} \mathrm{d}w \int_0^{w} S(v) \cos\left(2ka \sin\theta \sin\frac{w}{\sqrt{2}} \sin\frac{v}{2}\right) \mathrm{d}v \quad (2)$$

was obtained for calculating the radiation power scattered into the unit angle at the angle θ to the propagation direction of probe radiation. Here, k is the wave number; σ is the root-mean-square fluctuation amplitude; a is the core radius; $\Delta = \Delta n/n_0$ is the relative refractive index of the fibre core; n_0 is the refractive index of silica; c is the speed of light; E_a is the electric field strength at the core–cladding interface; L is the length in the fibre region from which scattered radiation is collected; $T(\theta)$ is the factor taking into account the capture of radiation in the fibre core;

$$R(u) = \exp(-u^2/L_c^2), \quad (3)$$

$$S(v) = \exp(-v^2/V_c^2) \quad (4)$$

are the normalised autocorrelation functions of deviations in the axial and azimuthal directions, respectively.

By using this model, we can compare the calculated and measured angular distributions of the scattered radiation intensity. For this purpose, we studied a Ge303sm step-index fibre ($\Delta n = 0.034$). The central dip in the index profile was virtually eliminated during preform fabrication (see inset in Fig. 4). The cut-off wavelength for the second mode in this fibre was 1.0 μm (the core diameter was ~ 2.5 μm), and the Ge303sm fibre was single-mode at the wavelength 1.064 μm at which measurements were performed. Figure 4 shows the measured and calculated scattering indicatrix for the Ge303sm fibre. The curve of the scattering indicatrix is formed by two terms corresponding to Rayleigh scattering (1) and anomalous scattering (2). The level of Rayleigh scattering and parameters L_c and V_c in expressions (3) and (4) were selected to obtain the best agreement between the calculated and measured curves.

The calculations show good agreement between the theoretical and experimental curves for the Ge303sm fibre with typical sizes of fluctuations in the axial (L_c) and azimuthal (V_c) directions equal to 0.46 μm, and 1.4 rad, respectively. The scatter of points at small angles (0–15°) in the measured scattering indicatrix is caused by interference whose modulation amplitude and period decrease with increasing the scattering angle. Some difference between the measured (averaged) and calculated indicatrices is observed only at small angles to the fibre axis where the radiation scattered at the core–cladding interface is partially captured in the fibre core. This effect was neglected in the calculation of the theoretical curve for anomalous scattering (it was assumed that $T(\theta) = 1$ for all θ). The scattering indicatrices of other fibres studied in the paper had a similar shape and were also well described by the sum of Rayleigh and anomalous scattering.

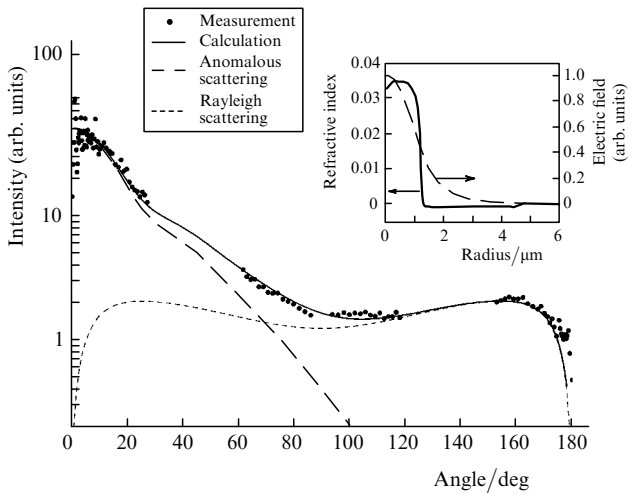

Figure 4. Comparison of the measured and calculated scattering indicatrices in the Ge303sm fibre. The inset shows the refractive index profile of the fibre and the radial distribution of the mode field.

3.3 Spectral dependence of optical losses at the core–cladding interface

The model of anomalous scattering [24] that we use here allows us to determine the spectral dependence of optical losses caused by scattering at the core–cladding interface. As follows from our calculations, this dependence is close to a power one, and the exponent of this dependence for parameters L_c and V_c describing anomalous scattering in the Ge303sm fibre is close to -3.

The spectral dependence of optical losses at the core–cladding interface can be also determined experimentally. The average losses at the core–cladding interface in the few-mode spectral region of the fibre were estimated by the method of differential mode losses in [22]. The estimates were performed for the Ge303sm fibre at the wavelength 632.8 nm of a helium–neon laser. As the core–cladding interface, the region of radii 1.05 – 1.3 μm was considered. In this region the refractive indices of the core glass at the distance r from the fibre axis $n(r)$ satisfies the relation $0.1\Delta n_{max} < \Delta n(r) < 0.9\Delta n_{max}$, where $\Delta n(r) = n(r) - n_0$ and n_0 is the refractive index of silica. The choice of such region as the core–cladding interface was conventional to a great extent, the only important factor being that the electric field strength of the fundamental mode in this region changed weakly (less than by 50 %), which allowed the averaging of optical losses in this region. The measurements showed that average optical losses at the interface were 288 dB km^{-1}.

The average optical losses at the interface can be also estimated in the spectral region where the Ge303sm fibre is single-mode. For this purpose, we subtracted optical losses caused by fundamental mechanisms (calculated from the results obtained in [8, 17–20]) from the spectrum of total optical losses, determining in this way the excess optical losses related to the core–cladding interface, as shown in [22]. As in [22], the region of radii 1.05–1.3 μm was considered conventionally as the core–cladding interface. By taking into account the fraction of power propagating in this region, we calculated the average optical losses in it. The results of this calculation for the wavelengths 1050–1600 nm and optical losses at the core–cladding interface calculated by the method of differential mode losses at a wavelength of 632.8 nm are shown in Fig. 5. One can see that the experimental spectral dependence well agrees with the dependence calculated above. Note that these estimates cover a rather broad spectral region (632–1600 nm), which demonstrates a high accuracy of the results.

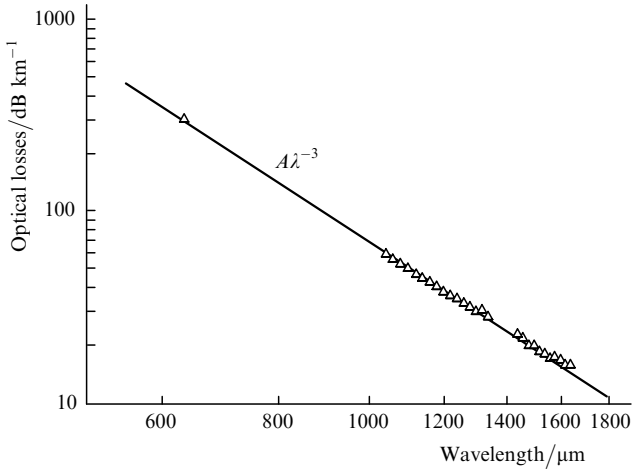

Figure 5. Spectral dependence of average optical losses at the core–cladding interface in the Ge303sm fibre; triangles are the calculation based on the measurements of total optical losses and differential mode losses; the solid curve is calculated by using the model [24].

4. Discussion of results

The study performed in the paper showed that a high level of optical losses in heavily doped germanosilicate single-mode fibres is caused by anomalous scattering with the indicatrix that substantially differs from that of Rayleigh scattering. Our previous results [22] allow us to conclude that anomalous scattering appears in the fibre core–cladding interface. Therefore, it is reasonable to assume that this mechanism of optical losses is caused by scattering of radiation from geometrical fluctuations of this interface along the fibre length, as was predicted theoretically in [23, 24]. The model developed in [23, 24] indeed well describes both the scattering indicatrix and the spectral dependence of optical losses at the core–cladding interface.

The question of the physical mechanism giving rise to geometrical fluctuations of the core–cladding interface and of variations in their amplitude along the fibre core remains open. One can assume that these perturbations are produced during the fabrication of fibre preforms. The distortion of the core–cladding interface called 'viscosity fingers' in [25] was indeed observed in [25, 26]. This effect appearing at the stage of the preform collapse can be explained either by the insufficiently high temperature of a support tube [26] or a great difference in the viscosities of the fibre core and cladding glasses [25]. At the same time, the assumption that the distortions of the core–cladding interface are produced at the stage of preform fabrication cannot explain a very strong dependence of optical losses on the fibre drawing conditions. As follows from our studies (see section 3.1), the total optical losses and anomalous scattering losses can change by more than three times upon increasing the fibre tension during drawing from 30 to 150 g. Such a strong correlation between the fibre drawing conditions and the value of anomalous scattering losses suggests that fluctuations of the core–cladding interface along the fibre length appear during the fibre drawing. In this case, the initial variations in the preform geometry can further grow during fibre drawing. It seems that this process occurs in the neck-down region – the region where the preform is stretched to a fibre and the preform glass is heated up to the maximum temperature and becomes the least viscous.

It is known that the interface of liquids with different viscosities is unstable when an external pressure is applied [27] and upon the movement of the interface along its normal [25]. It is such a situation that takes place during fibre drawing process: the viscoelastic flowing of the softened core and cladding glasses occurs both in the radial (the waist coefficient is 100–300) and axial (the waist coefficient is $10^4 - 10^5$) directions. The different thermal expansion coefficients and different softing temperatures of the core and cladding glasses (caused by different doping levels of the fibre core and cladding) give rise to stresses at the core–cladding interface during glass cooling [13, 14]; in this case, the viscosities of the fibre core and cladding also considerably differ [28, 29]. As a result, the size and shape of the core–cladding interface can fluctuate.

The relation of the increase in the intensity of anomalous scattering (and, correspondingly, in the amplitude of fluctuations of the core-cladding interface) with the difference in the viscosities of the core and cladding glasses during fibre drawing, as well as with their absolute viscosity is confirmed by a number of the following experimental facts:

(i) The increase in the concentration of germanium oxide in the fibre core reduces the core viscosity during drawing and, thereby increases the difference in the viscosities of the core and cladding glasses. As shown above, the increase in the molar concentration of GeO_2 in the core from 17 % to 27 % (change in Δn from 0.025 to 0.040) results in a considerable increase in the anomalous scattering intensity and, hence, in variations of the transverse dimensions of the fibre core.

(ii) The authors of paper [29] have found that the compensation of the difference of viscosities of the fibre core and cladding (selection of the compositions of the reflecting cladding and core to make their viscosities equal during fibre drawing) reduces optical losses even in the case of weakly doped phosphosilicate fibres.

(iii) Studies described in section 3.1 have shown that the level of optical losses caused by anomalous scattering depends to a great extent on the fibre drawing conditions. In this case, optical losses due to anomalous scattering are determined not by the temperature of a heater or the drawing rate but by the fibre tension during its drawing. As follows from the study of the drawing process [30], the fibre tension is directly related with the preform glass viscosity during drawing in the region of maximal heating.

(iv) We have shown earlier [6, 12] that total optical losses and anomalous scattering losses in single-mode graded-index fibres are considerably lower than those in step-index fibres at the same concentration of germanium oxide. Fibres of these two types differ from each other, in particular, in that there is no a sharp jump in the viscosity at the core–cladding in graded-index fibres during drawing.

All the facts presented above suggest that anomalous scattering is caused by fluctuations in the size and shape of the core–cladding interface produced due to the hydrodynamic instability of the interface of core and cladding glasses with different viscosities during fibre drawing.

5. Conclusions

We have studied the radiation scattering indicatrix for heavily doped single-mode fibres in a broad angular range and have found that anomalous scattering makes the

dominant contribution to the level of optical losses in these fibres. The analysis of the scattering indicatrix shape and spectral dependence of optical losses at the core–cladding interface has shown that anomalous scattering is caused by scattering from fluctuations of the core–cladding interface along the fibre length. The mechanism of these fluctuations has been proposed which assumes the development of the hydrodynamic instability of the interface of core and cladding glasses with different viscosities during fibre drawing from a preform.

References

1. Okuno T., Onishi M., Kashiwada T., Ishikawa S., Nishimura M. *IEEE J. Sel. Top. Quantum Electron.*, **5**, 2181 (1999).
2. Sudo S., Itoh H. *Opt. Quantum Electron.*, **22**, 187 (1990).
3. Davey S.T., Williams D.L., Spirit D.M., Ainslie B.J. *Proc. SPIE Int. Soc. Opt. Eng.*, **1171**, 181 (1989).
4. Abramov A.A., Bubnov M.M., Dianov E.M., Semenov S.L., Schebunjaev A.G., Guryanov A.N., Khopin V.F. *Proc. XVII Intern. Congr. on Glass* (Beiging, 1995) Vol. 7, p. 70.
5. Bubnov M.M., Semjonov S.L., Likhachev M.E., Dianov E.M., Khopin V.F., Salganskii M.Yu., Guryanov A.N., Fajardo J.C., Kuksenkov D.V., Koh J., Mazumder P. *Proc. ECOC-IOOC* (Italy, Rimini, 2003) Vol. 2, p. 212.
6. Bubnov M.M., Semjonov S.L., Likhachev M.E., Dianov E.M., Khopin V.F., Salganskii M.Yu., Guryanov A.N., Fajardo J.C., Kuksenkov D.V., Koh J., Mazumder P. *IEEE Photon. Technol. Lett.*, **16**, 1870 (2004).
7. Ohashi M., Shiraki K., Tajima K. *J. Lightwave Techn.*, **10**, 539 (1992).
8. Shibata N., Kawachi M., Edahiro T. *Trans. IECE Jpn*, **E 63**, 837 (1980).
9. Rawson E.G. *Appl. Opt.*, **11**, 2477 (1972).
10. Guenot P., Nouchi P., Poumellec B. *OFC'99 Techn. Dig.* (San-Diego, Cal., 1999, ThG2-1) p. 84.
11. Lines M.E., Reed W.A., Di Giovanni D.J., Hamblin J.R. *Electron. Lett.*, **35**, 1009 (1999).
12. Likhachev M.E., Bubnov M.M., Semenov S.L., Shvetsov V.V., Khopin V.F., Gur'yanov A.N., Dianov E.M. *Kvantovaya Elektron.*, **33**, 633 (2003) [*Quantum Electron.*, **33**, 633 (2003)].
13. Ainslie B.J., Beales K.J., Cooper D.M., Day C.R., Rush J.D. *J. Non-Cryst. Sol.*, **47**, 243 (1982).
14. Kajioka H., Kumagai T., Ishikawa T., Teraoka T. *Proc. OFC'88* (New Orlean, 1988, WI3) p. 75.
15. Belov A.V., Guryanov A.N., Devyatykh G.G., Dianov E.M., Khopin V.F., Kurkov A.S., Mashinsky V.M., Miroshnichenko S.I., Neustruev V.B., Vechkanov N.N. *Sov. J. Lightwave Commun.*, **2**, 281 (1992).
16. Dianov E.M., Kurkov A.S., Mashinsky V.M., Neustruev V.B., Guryanov A.N., Devyatykh G.G., Khopin V.F., Miroshnichenko S.I., Vechkanov N.N. *OFC/IOOC'93 Techn. Dig.* (San Jose, Cal., 1993, TuL1) p. 51.
17. Tsujikawa K., Ohashi M., Shiraki K., Tateda M. *Electron. Lett.*, **30**, 351 (1994).
18. Guenot P.L., Nouchi P., Poumellec B., Mercereau O. *Intern. Wire & Cable Proc.* (Eatontown, N.J., 1996) p. 679.
19. Likhachev M.E., Semenov S.L., Khopin V.F., Salganskii M.Yu., Zen'kovskii G.V., Bubnov M.M. *Electronic Journal 'Issledovano v Rossii' (Studied in Russia)*, **8**, 67 (2005); http://zhurnal.ape.relarn.ru/articles/2005/008.pdf.
20. Schultz P.C. *Proc. XI Intern. Congress on Glass* (Prague, 1977) Vol. 3, p. 155.
21. Fermann M.E., Poole S.B., Payne D.N., Martinez F. *J. Lightwave Techn.*, **6**, 545 (1988).
22. Likhachev M.E., Bubnov M.M., Semenov S.L., Khopin V.F., Salganskii M.Yu., Gur'yanov A.N., Dianov E.M. *Kvantovaya Elektron.*, **34**, 241 (2004) [*Quantum Electron.*, **34**, 241 (2004)].
23. Rawson E.G. *Appl. Opt.*, **13**, 2370 (1974).
24. Mazumder P., Logunov S., Raghavan S. *J. Appl. Phys.*, **96**, 4042 (2004).
25. Biryukov A.S., Dianov E.M., Kurkov A.S., Devyatykh G.G., Guryanov A.N., Gusovskii D.D., Kobis S.V. *Proc. ECOC'96* (Oslo, Norway, 1996, TuP.02) p. 2.225.
26. McNamara P., Lyytikainen K.J., Ryan T., Kaplin I.J., Ringer S.P. *Opt. Commun.*, **230**, 45 (2004).
27. Hunt G.W., Muhlhaus H.-B., Whiting A.I.M. *Phil. Trans. R. Soc. Ldn. A*, **355**, 2197 (1997).
28. Tajima K., Tateda M., Ohashi M. *J. Lightwave Tech.*, **12**, 411 (1994).
29. Tajima K., Tateda M., Ohashi M. *OFC'94 Tech. Dig.* (San Jose, Cal., 1994, TuB2) p. 2.
30. Paek U.C., Schoeder C.M., Kurkjian C.R. *Glass Technol.*, **29**, 263 (1988).